Biochemical and Biophysical Research Communications **289,** 125–129 (2001)
doi:10.1006/bbrc.2001.5931, available online at http://www.idealibrary.com on IDEAL®

Thermal Stability of Human Ferritin: Concentration Dependence and Enhanced Stability of an N-Terminal Fusion Mutant

Sung-Woo Kim, Yang-Hoon Kim, and Jeewon Lee[1]

Laboratory of Biomolecular Process Engineering, Korea Research Institute of Bioscience and Biotechnology (KRIBB), P.O. Box 115, Yusong, Taejon 305-600, South Korea

Received October 12, 2001

Though human L-chain ferritin has been known to be more resistant to physical denaturation than H-type ferritin, its stability characteristics and kinetic information have not been reported in detail. Overexpressed recombinant ferritin (FTN) in *Escherichia coli* formed inclusion bodies through noncovalent molecular interaction and easily dissolved with regaining the iron-uptake activity by a simple pH-shift process at high protein concentration (>600 mg l^{-1}). FTN was relatively thermostable at low protein concentration (0.2 g l^{-1}), but it became extremely thermolabile at high protein concentration (1.3 g l^{-1}), i.e., more than 80% of FTN was coprecipitated within 5 min under the same heat-induced denaturation condition. Aggregation rate constant for initial 5 min at high protein concentration was 6.04 × 10^{-3} s^{-1} for FTN. Surprisingly, glucagon · ferritin mutant (GFTN), consisting of an N-terminus fusion partner, human glucagon (29-residue α-helical peptide), showed significantly enhanced thermal stability even at high protein concentration. That is, in spite of 40-min heat treatment, more than 50% of GFTN the still remained soluble with maintaining the same functional properties. The aggregation rate constants were 2.75 × 10^{-4} and 2.80 × 10^{-4} s^{-1} at low and high concentration, respectively, for GFTN. These results suggest a critical participation of the N-terminal domain of ferritin in the temperature-induced aggregation pathway. Presumably, partially denatured amino terminus of FTN is involved in nonspecific molecular interaction resulting in the off-pathway aggregation. It is notable that the purified GFTN showed the same molar capacity of iron (Fe^{+3}) storage as standard ferritin. From the analysis of fluorescence emission spectrum, the physical stability of GFTN was also very comparable to that of standard ferritin under the various denaturation conditions induced by GdnHCl. © 2001 Academic Press

[1] To whom correspondence should be addressed: Fax: +82-42-860-4594. E-mail: jwlee@mail.kribb.re.kr.

Key Words: **ferritin; thermal stability; N-terminal fusion mutant; temperature-induced aggregation; N-terminal domain.**

An iron-storage protein, ferritin is a spherical shell consisting of 24 H- and L-chain subunits, and its shell structure is uniquely well designed to contain large amount of iron (1–4). Each subunit of ferritin is a bundle of four long α helices, with a fifth short helix, a short nonhelical extension at the C and N termini (1, 3). Biochemical studies of human H- and L-type chains and of some variants indicated that; (i) *in vitro* the H-chain ferritin oxidizes iron at rates several-fold faster than L-chain ferritin (5–9); (ii) L-chain ferritin appears to induce iron mineralization with higher efficiency than the H chain (10); and (iii) L chain is notably more stable to physical denaturation than H-type ferritin (11).

Santambrogio *et al.* (1993) reported that soluble recombinant human ferritin was produced using λ_{pL} promoter system in *E. coli*, but the production level was quite low, i.e., 10–15 mg and 2–5 mg per liter of culture for H- and L-chain human ferritins, respectively. Reportedly, x-ray analyses of recombinant ferritins expressed in *E. coli* showed H and L chains to have homologous subunit conformations and subunit arrangements (3, 13, 14). The unfold recombinant human ferritin by guanidine denaturation was renatured to form homomutimeric multimers indistinguishable from the native ones (12), and the Gdn-HCl denaturation and renaturation characteristics were compared between H- and L-chain ferritins (12). Especially with human H-chain ferritin, its ferroxidase function, and stability characteristics were extensively studied, and a detailed mutation study showed that the carboxyl terminus of H-chain ferritin is of crucial importance in the formation of stable iron core (5).

0006-291X/01 $35.00

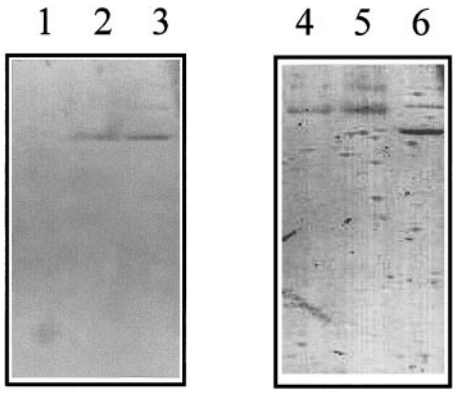

FIG. 1. Prussian-blue-stained polyacrylamide gels (native-PAGE) of FTN and GFTN protein samples after pH-shift dissolution of recovered inclusion bodies: lane 1, bovine serum albumin (negative control); lane 2, FTN; lane 3, standard ferritin; lanes 4 and 5, GFTN loaded by different amounts (13 and 26 μg, respectively); lane 6, standard ferritin.

As confirmed in the present study, high-level expression of recombinant human L-chain ferritin using T7 promoter system resulted in the formation of inclusion bodies. Interestingly, the recombinant ferritin aggregates were easily dissolved by a simple pH-shift process and simultaneously renatured with gaining the iron uptake activity. In contrast to the efficient pH-shift renaturation, the renatured recombinant L-chain ferritin was extremely thermolabile at high protein concentration. Since the stability characteristics of human L-chain ferritin have not been studied in detail yet, it would provide useful information for better understanding of the stability nature to investigate the aggregation kinetics of human L-chain ferritin and its fusion mutant. In this study, we developed a recombinant fusion mutant of human L-chain ferritin by placing 29-residue glucagon peptide at the N-terminus. The fusion mutant was also efficiently renatured by the simple pH-shift, but surprisingly, the presence of the additional peptide at the amino terminus significantly increased the thermal stability of L-chain ferritin by enhancing the kinetic barriers in the denaturation pathway. Physical stabilities of the fusion mutant under guanidine-induced denaturation conditions and iron-storage capacity have been also demonstrated in detail and compared with the properties of directly-expressed and/or standard ferritins.

MATERIALS AND METHODS

Recombinant strains and gene expression. Human ferritin (L-chain) gene was cloned from human liver cDNA library (Clontech, CA). After PCR-amplification using appropriate primers, the human ferritin gene was inserted into the *Nde*I–*Hin*dIII site of plasmid pT7-7 (15) to construct expression vector pT7-Fer for the direct expression of human ferritin. The FTN gene was also inserted into *Xho*I–*Hin*dIII site of plasmid pG-IL2 (16) to construct expression vector pT7-GFer for the synthesis of recombinant fusion mutant, GFTN. After complete DNA sequencing of all plasmid vectors purified, the *E. coli* strain BL21(DE3) (F^- *omp*T *hsd*S_B(rB^-mB^-)) was transformed with the constructed plasmid vectors above, and ampicillin-resistant transformants were selected. For the shake flask experiments (250 ml Erlenmeyer flasks, 37°C, 200 rpm), LB media containing 100 mg ampicillin per liter of culture was used. When the culture $O.D._{600}$ reached 0.4, the gene expression was induced by adding IPTG (0.5 mM), and the induced cultures were harvested after further 3–4 h cultivation. The recombinant cells in 50 ml culture were spun down at 6000 rpm for 5 min, and the cell pellets were resuspended in 5 ml distilled water. After cell disruption by using Branson Sonifier (Branson Ultrasonics Corp., Danbury, CT), the insoluble protein aggregates were isolated at 13,000 rpm for 10 min, washed twice with 1% Triton X-100, and subject to reducing or non-reducing SDS–PAGE analysis.

Renaturation of inclusion bodies and heat treatment. The recovered inclusion bodies were subsequently dissolved (0.6–1 g/L) in 5 ml alkaline solution (pH 12) without adding any denaturing agents. After 2 min, the solution pH was quickly shifted back to 8 by adding 1 M Tris–HCl buffer, pH 8. After centrifuge (13,000 rpm for 10 min) the soluble proteins and insoluble aggregates in 50 mM Tris–HCl buffer were analyzed by native-PAGE or SDS–PAGE. Dissolved recombinant proteins were subject to heat treatment at 72°C for 50 min, and then after centrifuge (13,000 rpm for 10 min) the soluble FTN and GFTN in various time-course samples were analyzed by native-PAGE and reducing SDS–PAGE.

Estimation of iron-storage capacity of recombinant proteins. Iron-storage capacities of standard ferritin (50 mg/L) and GFTN (50 mg/L) purified through the heat treatment process above, were examined by analyzing the amount of unbound free iron using ICP (inductively-coupled plasma) atomic emission spectrometry (IRIS/AP spectrometer, Thermo Jarrell Ash Corp., Franklin, USA) after incubated with ferric chloride (0.4 mM) at 4°C for 18 h. Standard ferritin was kindly provided by Dr. Paolo Arosio (Protein Engineering Unit, Dibit, H. San Raffaele, Milano, Italy).

Electrophoresis and spectrophotometric analyses for stability estimation. FTN, GFTN, and standard ferritin were subject to reducing (15 mM DTT) and nonreducing SDS–PAGE and native PAGE (14% Tris-glycine precast gel, Novex, San Diego, CA), followed by Coomassie, Silver, or Prussian-blue (10, 12) staining where applicable. The resulting protein bands were scanned and analyzed using a densitometer (Duoscan T1200, Bio-Rad, Hercules, CA).

Fluorescence spectra were collected with a Perkin–Elmer spectrofluorimeter with excitation window of 3 nm and emission window of 20 nm. Denaturation plot was obtained by incubating ferritin samples (50 mg/L) for 18 h at 4°C with various GdnHCl concentrations in 0.1 M phosphate buffer, pH 7.4 and 3 mM DTT. The conformational status of standard ferritin or GFTN was derived from fluorescence spectra with excitation at 295 nm, using as controls the ferritin in 0.1 M phosphate, pH 7.4 (native status), and in 6 M GdnHCl, 0.1 M phosphate buffer, pH 3.5 (denatured status). Fluorescence spectra were analyzed for the ratios of the emission at 355 and 330 nm.

RESULTS AND DISCUSSION

Renaturation of FTN and GFTN Produced in E. coli

In the SDS–PAGE analyses of inclusion bodies of FTN and GFTN, each recombinant protein appeared at monomer position under both reducing and non-reducing conditions (data not shown), and hence it seems that the intracellular aggregates were formed via noncovalent intermolecular linkages. More than 80% of the FTN and GFTN aggregates were quickly dissolved at high concentrations (0.6–1.0 g/L) by a

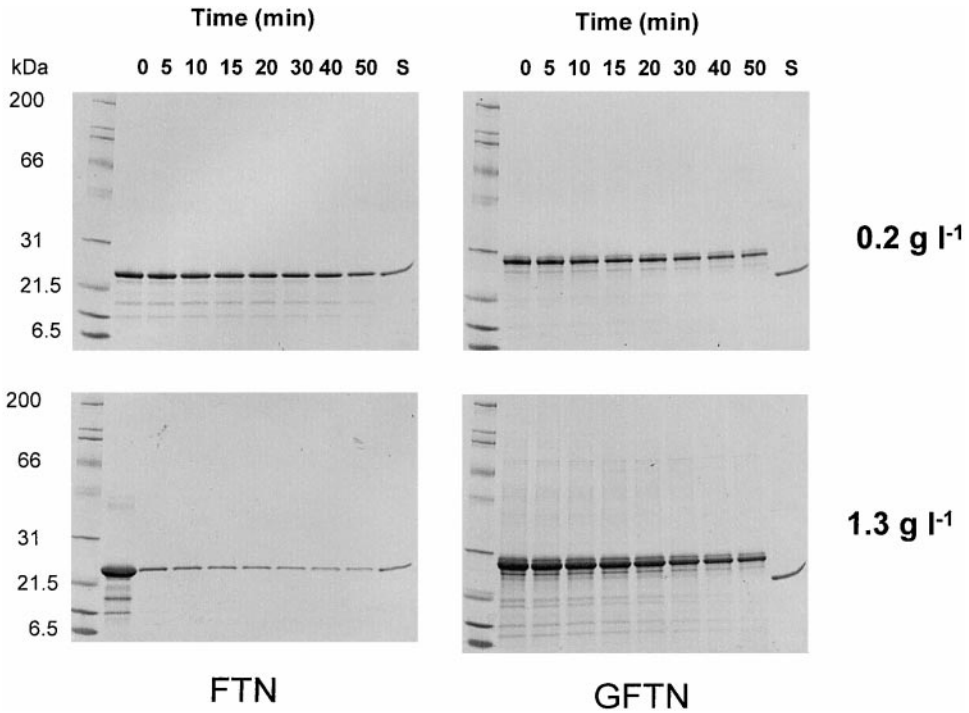

FIG. 2. Coomassie-stained polyacrylamide gels (reducing SDS–PAGE) of FTN and GFTN protein samples at different concentrations, 0.2 and 1.3 g l^{-1} during denaturation at 72°C. ("S" represents standard human L-chain ferritin.)

simple pH-shift process (8→12→8). Subsequently, the dissolved FTN and GFTN (50 mg/L) were subject to iron saturation experiment with 0.4 mM ferric chloride. The iron uptake of FTN and GFTN was confirmed through Prussian-blue gel staining after native-PAGE (Fig. 1). Notably in Fig. 1, both of FTN and GFTN were clearly stained as iron-bound proteins like standard ferritin while BSA (bovine serum albumin, negative control) was not stained at all. Consequently, through the simple pH-shift process, the insoluble FTN and GFTN aggregates were converted into active recombinant proteins with the same functional property as standard ferritin.

Aggregation Kinetics of FTN and GFTN

Figure 2 shows the rapid disappearing of soluble FTN at high protein concentration (1.3 g l^{-1}) under the temperature-induced denaturation condition, whereas the fusion mutant GFTN maintained high thermal sta-

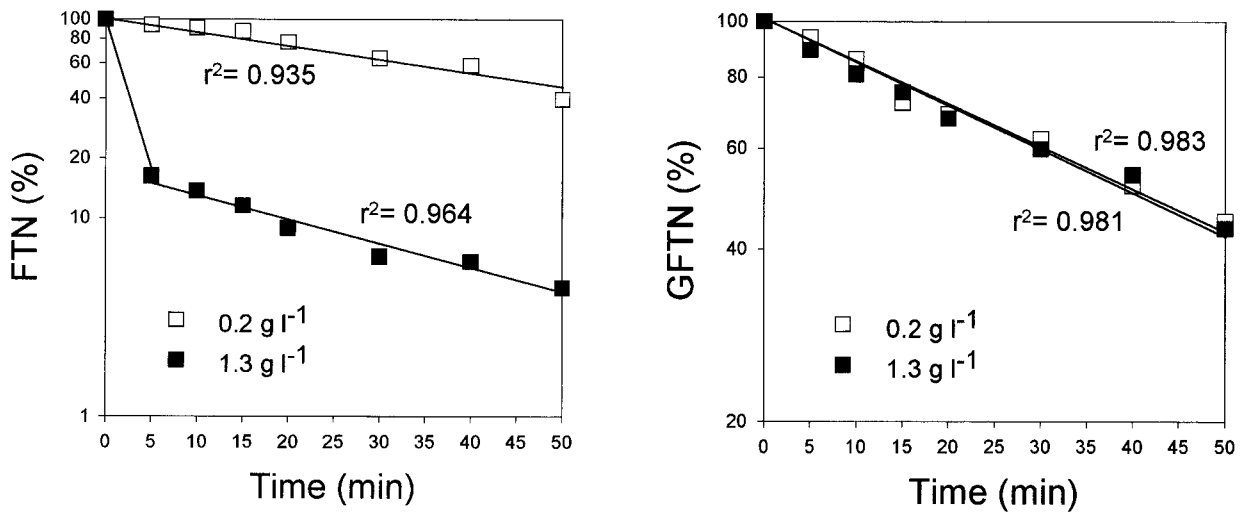

FIG. 3. Thermal denaturation kinetics of FTN and GFTN: Semi-logarithmic plot showing time-course aggregation of FTN and GFTN based on quantitative analysis of protein bands in Fig. 2. (r^2 represents correlation coefficient of each linearly-regressed line.)

TABLE 1

Aggregation Rate Constants (s^{-1}) of FTN and GFTN, k_H and k_L at Low (0.2 g l^{-1}) and High (1.3 g l^{-1}) Protein Concentration, Respectively, under Heat-Induced Denaturation Condition

Constant	Protein FTN	GFTN
k_L	2.60×10^{-4}	2.75×10^{-4}
k_H	[a] 6.04×10^{-3}	2.80×10^{-4}
	[b] 4.73×10^{-4}	

Note. At high protein concentration, most FTN aggregated rapidly within first 5 min, and afterwards the aggregation slowly progressed (Fig. 3), and hence in this case the aggregation rate constant was estimated separately in two different time periods, i.e., initial 5-min and next 45-min periods.

[a] Estimated for initial 5 min.

[b] Estimated for next 45 min.

bility at both high and low protein concentrations. The quantitative analysis of soluble FTN and GFTN bands allows the kinetic analysis of the aggregation process (Fig. 3) by finding the parameters of the equation that describes the time-dependent aggregation of FTN and GFTN: $dN/dt = -kN$ where N and k represent quantity of soluble protein (FTN or GFTN) and aggregation rate constant, respectively. The first-order kinetic equation above was used because the results of time-course aggregation were well fitted by linear regression in the semi-logarithmic plot as shown in Fig. 3. The

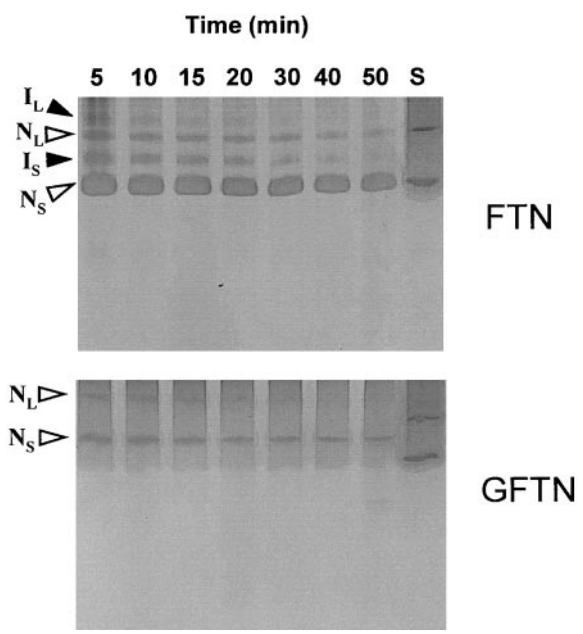

FIG. 4. Silver-stained polyacrylamide gels (native-PAGE) of FTN and GFTN samples during denaturation at 72°C at high protein concentration (1.3 g l^{-1}). N_S and N_L indicate native multimers of FTN and GFTN, and I_S and I_L represent presumed partially-unfolded forms of N_L and N_S of FTN, respectively. ("S" represents standard human L-chain ferritin.)

TABLE 2

Iron (Fe^{+3}) Storage Capacity of Standard Ferritin and GFTN Purified through Heat Treatment Process

Protein	Molar iron (Fe^{+3}) storage capacity
Standard ferritin	123 moles Fe^{+3} per mole subunit
GFTN	128 moles Fe^{+3} per mole subunit

rate constants for FTN and GFTN at different protein concentration are shown in Table 1. Note that the amino terminal fusion of glucagon exhibits more than 20-fold reduction in the initial aggregation rate at high protein concentration, compared to the aggregation of FTN. The aggregation rate constant for GFTN is nearly invariable despite the significant change of protein concentration (Fig. 3 and Table 1). Therefore, the presence of the fused glucagon peptide at the amino terminus seems to engender a kinetic barrier preventing the off-pathway aggregation, probably caused by the imposition of steric impediments to the denaturation process that initiates at the amino terminus of FTN. Time-course unfolding process at high protein concentration (1.3 g l^{-1}) was also analyzed using native-PAGE as shown in Fig. 4. Standard L-chain ferritin shows two major multimers, i.e., N_S and N_L in silver-stained polyacrylamide gels. In native-PAGE of FTN, two additional proteins, I_S and I_L appear at early stage of aggregation process and gradually disappeared, while in the denaturation process of GFTN no additional protein bands are shown besides two major native multimers. Since FTN showed high thermal instability at high protein concentration (Fig. 3), it is likely that I_S and I_L are partially unfolded intermediates of N_S and N_L, respectively, in the aggregation pathway activated at high protein concentration. I_S and I_L still seem to form large multimers (showing slower migration than N_S and N_L, respectively, in native PAGE), which probably happened because prior to complete dissociation of the subunits, the amino terminus of FTN polypeptide chain starts to be partially denatured first while the rest of the polypeptide still interacts with other polypeptide chains with maintaining multimeric forms. This partially denatured FTN may be involved in nonspecific molecular interaction resulting in off-pathway aggregation. Figure 4 shows that this partial denaturation of FTN is effectively prevented by the amino terminus peptide fusion, that is, the α-helical glucagon is completely interwound so that subunit dissociation cannot occur without substantial denaturation, which is probably a major reason for the high thermal stability of GFTN. These observations confirm the critical role of the FTN amino terminal domain in the initiation of protein aggregation process during the heat-induced denaturation and may provide interesting information to further

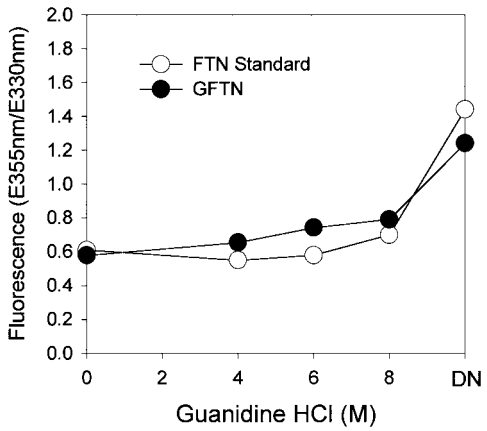

FIG. 5. Denaturation plot of standard ferritin (50 mg l^{-1}) and GFTN (50 mg l^{-1}) purified through heat treatment process monitored by the ratio of fluorescence emission at 355 and 330 nm with excitation at 295 nm.

explore unfolding kinetics of this multimeric and unstable protein.

Characteristics of GFTN Function and Physical Stability

GFTN was purified through the repeated heat treatment process at low protein concentration, and its iron-storage capacity was analyzed and compared with that of standard ferritin. Table 2 shows that the molar iron-storage capacities of GFTN and standard ferritin were very comparable, indicating GFTN has the same functional property as the standard ferritin.

The purified GFTN and standard ferritin were denatured under various denaturation conditions generated by adding GdnHCl (4–8 M) in 0.1 M phosphate buffer (pH 7.4). Fully-denatured status ("DN" in Fig. 5) was achieved in 6 M GdnHCl, 0.1 M phosphate buffer (pH 3.5), as previously reported by Santambrogio *et al.* (1993). Fluorescence emission spectrum of each denatured sample was analyzed using Perkin–Elmer spectrofluorimeter at the excitation at 295 nm, and the ratios of the emission at 330 and 355 nm were estimated. Protein stability probed by the variation in fluorescence of samples under the Gdn-HCl-induced denaturation conditions shows that GFTN has very comparable physical stability as the standard ferritin (Fig. 5).

Protein GFTN, in which a foreign peptide (glucagons) is fused at the amino terminus of FTN, is the firstly described example of a new type of FTN mutants, showing an dramatic increase of its thermal stability, or decrease in the aggregation rate without interrupting the intrinsic functional property (i.e., iron-uptake activity) of FTN.

ACKNOWLEDGMENTS

This work has been supported by BBRC (Bioproducts & Biotechnology Research Center) of MOST (Ministry of Science and Technology) in Republic of Korea.

REFERENCES

1. Ford, G. C., Harrison, P. M., Rice, D. W., Smith, J. M. A., Treffry, A., White, J. L., and Yariv, J. (1984) Ferritin: Design and formation of an iron-storage molecule. *Philos. Trans. R. Soc. Lond. B Biol. Sci.* **304,** 551–565.
2. Theil, E. C. (1987) Ferritin: Structure, gene regulation, and cellular function in animals, plants, and microorganisms. *Annu. Rev. Biochem.* **56,** 289–315.
3. Harrison, P. M., Ford, G. C., Rice, D. W., Smith, J. M. A., and Treffry, A. (1987) Structural and functional studies on ferritins. *Biochem. Soc. Trans.* **15,** 744–748.
4. Aisen, P., and Listowsky, I. (1980) Iron transport and storage proteins. *Annu. Rev. Biochem.* **49,** 357–393.
5. Levi, S., Luzzago, A., Cesareni, G., Cozzi, A., Franceschinelli, F., Albertini, A., and Arosio, P. (1988) Mechanism of ferritin iron uptake: Activity of the H-chain and deletion mapping of the ferro-oxidase site. A study of iron uptake and ferro- oxidase activity of human liver, recombinant H-chain ferritins, and of two H-chain deletion mutants. *J. Biol. Chem.* **263,** 18086–18092.
6. Levi, S., Salfeld, J., Franceschinelli, F., Cozzi, A., Dorner, M. H., and Arosio, P. (1989) Expression and structural and functional properties of human ferritin L-chain from *Escherichia coli. Biochemistry* **28,** 5179–5184.
7. Cozzi, A., Santambrogio, P., Levi, S., and Arosio, P. (1990) Iron detoxifying activity of ferritin. Effects of H and L human apoferritins on lipid peroxidation *in vitro. FEBS Lett.* **277,** 119–122.
8. Lawson, D. M., Treffry, A., Artymiuk, P. J., Harrison, P. M., Yewdall, S. J., Luzzago, A., Cesareni, G., Levi, S., and Arosio, P. (1989) Identification of the ferroxidase centre in ferritin. *FEBS Lett.* **254,** 207–210.
9. Wade, V. J., Levi, S., Arosio, P., Treffry, A., Harrison, P. M., and Mann, S. (1991). Influence of site-directed modifications on the formation of iron cores in ferritin. *J. Mol. Biol.* **221,** 1443–1452.
10. Levi, S., Santambrogio, P., Cozzi, A., Rovida, E., Albertini, A., Yewdall, S. J., Harrison, P. M., and Arosio, P. (1992) Evidence of H- and L-chains have cooperative roles in the iron-uptake mechanism of human ferritin. *Biochem. J.* **288,** 591–596.
11. Santambrigio, P., Levi, S., Arosio, P., Palagi, L., Vecchio, G., Lawson, D. M., Yewdall, S. J., Artymiuk, P. J., Harrison, P. M., Jappelli, R., and Cesareni, G. (1992) Evidence that a salt bridge in the light chain contributes to the physical stability difference between heavy and light human ferritins. *J. Biol. Chem.* **267,** 14077–14083.
12. Santambrigio, P., Levi, S., Cozzi, A., Rovida, E., Albertini, A., and Arosio, P. (1993) Production and characterization of recombinant heteropolymers of human ferritin H and L chains. *J. Biol. Chem.* **268,** 12744–12748.
13. Lawson, D. M. (1990) X-ray Structure Determination of Recombinant Ferritins. Ph. D. thesis, University of Sheffield, Sheffield, United Kingdom.
14. Lawson, D. M., Artymiuk, P. J., Yewdall, S. J., Livingstone, J. C., Treffry, A., Luzzago, A., Levi, S., Arosio, P., Cesareni, G., Thomas, C. D., Shaw, W., and Harrison, P. M. (1991) Solving the structure of human H ferritin by genetically engineering intermolecular crystal contacts. *Nature* **349,** 541–544.
15. Tabor, S., and Richardson, C. C. (1985) A bacteriophage T7 RNA polymerase/promoter system for controlled exclusive expression of specific genes. *Proc. Natl. Acad. Sci. USA* **82,** 1074–1078.
16. Kim, D.-Y., Lee, J., Saraswat, V., and Park, Y.-H. (2000) Glucagon-induced self-association of recombinant proteins in *Escherichia coli* and affinity purification using a fragment of glucagon receptor. *Biotechnol. Bioeng.* **69,** 418–428.